

Altered surface trafficking of presynaptic cannabinoid type 1 receptor in and out synaptic terminals parallels receptor desensitization

Lenka Mikasova^a, Laurent Groc^b, Daniel Choquet^{b,1}, and Olivier J. Manzoni^{a,1,2}

^aInstitut National de la Santé et de la Recherche Médicale U862 Laboratory Physiopathology of Synaptic Plasticity, Neurocentre Magendie, 146 rue Leo Saignat, 33077 Bordeaux, France; and ^bPhysiologie Cellulaire de la Synapse, Centre National de la Recherche Scientifique-Unité Mixte de Recherche 5091, Université Bordeaux 2, 33077 Bordeaux, France

Edited by Richard L. Huganir, Johns Hopkins University School of Medicine, Baltimore, MD, and approved October 8, 2008 (received for review June 20, 2008)

Presynaptic cannabinoid type 1 receptors (CB1Rs) are major mediators of retrograde synaptic plasticity at both excitatory and inhibitory synapses and participate in a plethora of physiological functions. Whether presynaptic receptors, such as CB1R, display functionally relevant movements at the surface of neuronal membranes is not known. We analyzed the lateral mobility of native CB1Rs in cortical neurons by using single-quantum dot imaging. We found that CB1Rs are highly mobile and rapidly diffuse in and out of presynapses. Agonist-induced desensitization correlated with a reduction in the fraction of surface CB1Rs and a drastic decrease in the membrane dynamic of the CB1Rs that remained at the presynaptic surface. Desensitization specifically excluded CB1Rs from synapses and increased the fraction of immobile receptors in the extrasynaptic compartment. The results suggest that decrease of mobility may be one of the core mechanisms underlying the desensitization of CB1R, the most abundant G protein-coupled receptor in the brain.

receptor mobility | CB1R | G-protein coupled receptor

Cannabinoid type 1 receptors (CB1Rs) and endocannabinoids (eCBs), as well as their synthesizing and degrading enzymes, constitute the eCB system (1, 2). In the CNS, the eCB system mediates retrograde signaling: postsynaptically produced eCBs cross the synapses and activate presynaptic CB1Rs (3). In addition to exocytosis/endocytosis, neurotransmitter receptor movement into and out of synapses may be one of the core mechanisms for rapidly changing the number of functional postsynaptic receptors (4, 5). Curiously, the lateral movements of presynaptic receptors, such as CB1Rs, have never been studied.

Determining whether CB1Rs diffuse in presynaptic membranes, similarly to postsynaptic ionotropic receptors (5), is necessary to understand the molecular logic of the eCB system (1). Because CB1Rs must be within reaching distance of eCBs to fulfill their presynaptic functions (3), surface diffusion potentially represents an efficient and rapid means of modulating retrograde signaling. CB1Rs are classical G protein-coupled receptors (GPCRs), and prolonged agonist treatment triggers both internalization via the clathrin-coated pit pathway (ref. 6, but see ref. 7) and uncoupling from their effector G proteins. A single in vivo exposure to Δ^9 -tetrahydrocannabinol abolishes eCB-mediated retrograde signaling and reduces the CB1R maximal efficacy without modifying total binding or coupling (8). Thus, another mechanism must exist to functionally desensitize CB1Rs in response to agonist exposure. A tantalizing hypothesis is that CB1Rs are moved away from their presynaptic site of actions following agonist exposure.

Here, we analyzed the surface mobility of native CB1Rs in cortical neurons in vitro by using single-quantum dot imaging (9). Our data support the idea that the dynamic exclusion of CB1Rs from a particular presynaptic subdomain might play a

prominent role in the desensitization of the most abundant GPCRs in the brain.

Results

CB1Rs Are Highly Mobile on the Surface of Cortical Neurons. Live staining of surface CB1Rs revealed that in cortical primary neurons (9–10 days in vitro) the vast majority of surface CB1R immunolabeling colocalizes with the axonal marker Tau1 (Fig. 1A). There was nearly no colocalization between the somatodendritic marker microtubule-associated protein 2 (MAP2) and CB1Rs, showing that surface CB1Rs are predominantly axonal in mouse cortical neurons in vitro. We colabeled for CB1R and glutamic acid decarboxylase 65 (GAD65), a marker of GABAergic neurons, and found that only $13\% \pm 1\%$ ($n = 603$) of all neurons were GAD65-positive. Moreover, $51\% \pm 11\%$ ($n = 89$) of CB1Rs were detected on GAD65-positive neurites [supporting information (SI) Fig. S1], suggesting that both glutamatergic and GABAergic cortical neurons express CB1Rs in vitro. Further analysis revealed that $66.1\% \pm 5.7\%$ ($n = 69$) of GAD65-positive neurons expressed CB1R immunolabeling and that $9.8\% \pm 1.6\%$ ($n = 346$) of non-GAD65-positive neurons expressed CB1R immunolabeling.

To specifically track surface CB1Rs in real time, polyclonal antibodies directed against an extracellular N-terminus domain of CB1R were coupled to anti-rabbit F(ab')₂ conjugated with Quantum Dots 655 nm (Qdots). Synapses were visualized with a fluorescent marker of active mitochondria, MitoTracker-Green, which colocalizes with presynaptic synaptotagmin clusters (10, 11). A real-time video of CB1R-Qdots recorded in 9- to 10-days-in-vitro cortical neurons (32°C) is available as [Movie S1](#). Instantaneous diffusion coefficient (D), percentage of mobile receptors, synaptic dwell time, percentage of synaptic receptors, and mean square displacement (MSD) were all calculated from reconstructed CB1R-Qdot trajectories.

In control conditions, surface CB1Rs displayed a high level of lateral mobility: $\approx 83\%$ were mobile (i.e., $D > 0.005 \mu\text{m}^2/\text{s}$) (Fig. 1C). Within synaptic and extrasynaptic compartments CB1Rs alternated between periods of diffusive movement (Fig. 1B).

How long do CB1Rs spend within the synapse? The synaptic dwell time of CB1Rs was 6 times shorter than that of postsynaptic

Author contributions: D.C. and O.J.M. designed research; L.M. performed research; L.G. and D.C. contributed new reagents/analytic tools; L.M. and L.G. analyzed data; and O.J.M. wrote the paper.

The authors declare no conflict of interest.

This article is a PNAS Direct Submission.

Freely available online through the PNAS open access option.

¹D.C. and O.J.M. contributed equally to this work.

²To whom correspondence should be addressed. E-mail: olivier.manzoni@inserm.fr.

This article contains supporting information online at www.pnas.org/cgi/content/full/0805959105/DCSupplemental.

© 2008 by The National Academy of Sciences of the USA

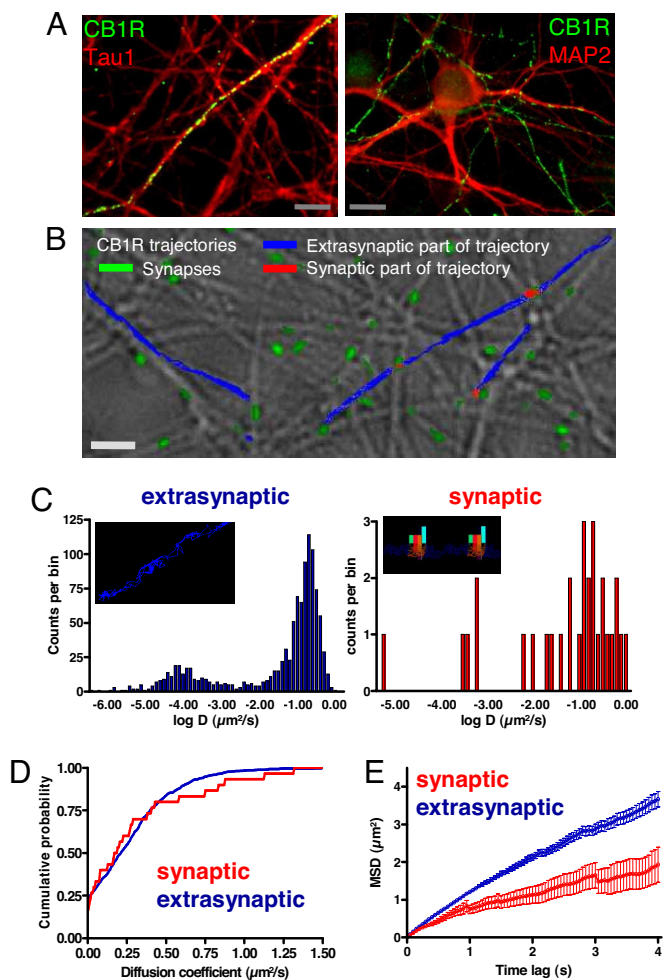


Fig. 1. CB1Rs are highly mobile on the surface of cortical neurons. (A) (Left) Merged images showing the colocalization (yellow) of CB1R (green) and of the axonal marker Tau1 (red). (Scale bar, 8 μm .) (Right) Nearly no colocalization was observed between the dendritic marker MAP2 (red) and CB1R (green). (Scale bar, 10 μm .) (B) Sample image of reconstructed CB1R-QD655 trajectories. Synapses were visualized with MitoTracker (green); the extrasynaptic part of CB1R trajectories is marked in blue, and the synaptic part in red. (Scale bar, 3 μm .) (C) Distribution of diffusion coefficient values of extrasynaptic (Left) and synaptic (Right) CB1Rs: about 83% of total CB1Rs were mobile. Bin size, 0.1 $\mu\text{m}^2/\text{s}$. Examples of CB1R extrasynaptic and synaptic trajectories with the color code used in B. (D) Synaptic and extrasynaptic receptors have similar distributions of diffusion coefficients (1,072 extrasynaptic trajectories and 30 synaptic trajectories). (E) Plot of the mean square displacement (MSD) of extrasynaptic and synaptic CB1Rs as a function of time. Synaptic CB1Rs have lower MSDs than the extrasynaptic CB1Rs. The diffusion of synaptic CB1Rs was closer to that of confined particles, whereas extrasynaptic CB1Rs freely diffused in neuronal membrane (583 extrasynaptic trajectories and 22 synaptic trajectories).

GluR2-containing AMPA receptors (AMPA; 0.2 ± 0.05 s, $n = 24$, and 1.3 ± 0.4 s, $n = 20$, respectively; see Fig. 4B) (12, 13), likely due to differences in the environment of presynaptic CB1Rs and postsynaptic GluR2-containing AMPARs.

A comparison of the distribution of diffusion coefficients of the global population of CB1Rs (i.e., mobile and immobile) revealed no difference between the mobility of synaptic and extrasynaptic CB1Rs [extrasynaptic: median = $0.213 \mu\text{m}^2/\text{s}$, interquartile range (IQR; 25–75%) = 0.019 – $0.405 \mu\text{m}^2/\text{s}$, $n = 1,072$; synaptic: median = $0.182 \mu\text{m}^2/\text{s}$, IQR = 0.02 – $0.42 \mu\text{m}^2/\text{s}$, $n = 30$; $P > 0.05$; Fig. 1D). Compared with other neurotransmitter receptors, the diffusion coefficients of CB1R and AM-

PAR were similar (14). Further analysis revealed that the distribution of the diffusion coefficients of mobile extrasynaptic and synaptic CB1Rs were identical (833 extrasynaptic CB1Rs: median = $0.297 \mu\text{m}^2/\text{s}$, IQR = 0.154 – $0.465 \mu\text{m}^2/\text{s}$; 25 synaptic CB1Rs: median = $0.225 \mu\text{m}^2/\text{s}$, IQR = 0.083 – $0.506 \mu\text{m}^2/\text{s}$; $P > 0.05$). Within the extrasynaptic subdomain, the MSD of extrasynaptic CB1Rs as a function of time was linear, indicating free diffusive movement (Fig. 1E). In contrast, the MSD values of CB1Rs within the spatially restricted synaptic subdomain reflected spatially confined movement (Fig. 1E).

Desensitization Dramatically Reduces the Fraction of Mobile CB1Rs. In rodents, subchronic activation of CB1Rs strongly desensitizes CB1Rs (15, 16). In animal and cellular models, CB1R desensitization is achieved easily by prolonged treatment with a CB1 agonist (17–19). Cortical neurons were treated with the synthetic cannabinoid agonist (*R*)-(+)-[2,3-dihydro-5-methyl-3-(4-morpholinylmethyl)pyrrolo[1,2,3-*de*]-1,4-benzoxazin-6-yl]-1-naphthalenylmethanone (WIN; 400 nM), the selective CB1 antagonist 1-(2,4-dichlorophenyl)-5-(4-iodophenyl)-4-methyl-*N*-4-morpholinyl-1*H*-pyrazole-3-carboxamide (AM281; 400 nM), or vehicle (0.1% DMSO) for 20 h. In agreement with previous reports (20, 21), 20 h of WIN treatment strongly reduced surface CB1Rs. There were 61.5 ± 12.2 ($n = 369$) and only 19.1 ± 2.2 ($n = 145$) CB1R-Qdots particles per observation field after 20 h of treatment with vehicle and WIN, respectively (*t* test, $P < 0.01$). Chronic WIN treatment dramatically lowered the diffusion coefficients of surface CB1Rs (control: median = $0.135 \mu\text{m}^2/\text{s}$, IQR = 0.055 – $0.232 \mu\text{m}^2/\text{s}$, $n = 369$; AM281: median = $0.157 \mu\text{m}^2/\text{s}$, IQR = 0.081 – $0.261 \mu\text{m}^2/\text{s}$, $n = 808$; and WIN: median = $0.074 \mu\text{m}^2/\text{s}$, IQR = 0.0001 – $0.183 \mu\text{m}^2/\text{s}$, $n = 145$; $P < 0.001$; Fig. 2A). The apparent reduction in the diffusion coefficients could be due to a reduction of the diffusion of mobile CB1Rs or an increase in the fraction of immobile CB1Rs. Our data support the second possibility. The diffusion coefficients of all mobile receptors were not significantly different across the different groups (control: median = $0.157 \mu\text{m}^2/\text{s}$, IQR = 0.09 – $0.251 \mu\text{m}^2/\text{s}$, $n = 320$; AM281: median = $0.168 \mu\text{m}^2/\text{s}$, IQR = 0.101 – $0.267 \mu\text{m}^2/\text{s}$, $n = 741$; and WIN: median = $0.152 \mu\text{m}^2/\text{s}$, IQR = 0.09 – $0.242 \mu\text{m}^2/\text{s}$, $n = 91$; $P > 0.05$). In contrast, prolonged treatment with the cannabinoid agonist led to a large increase in the fraction of immobile CB1Rs. Chronic incubation with AM281, a described antagonist with inverse agonist properties, had no effect on the fraction of immobile CB1Rs (Fig. 2B). After 20 h of treatment, the percentage of mobile CB1Rs was $83.0\% \pm 4.6\%$ ($n = 369$), $90.3\% \pm 1.9\%$ ($n = 808$), and $57.6\% \pm 8.6\%$ ($n = 145$) in control, AM281-treated, and WIN-treated neurons, respectively. Thus, the remarkable shift in the distribution of diffusion coefficients toward lower values observed after prolonged agonist exposure is due to an increase in the fraction of immobile receptors.

Moderate Desensitization Is Sufficient to Reduce CB1R Surface Mobility. We tested the effects of short agonist treatments on CB1R lateral mobility. Cortical neurons were incubated for 30 min or 2 h with the agonist WIN, the antagonist AM281, or vehicle. Thirty minutes of treatment had no consequence on CB1R mobility (Fig. S2). In contrast, a 2-h treatment with the cannabinoid agonist diminished CB1R mobility: the diffusion coefficients of all CB1Rs were lowered (control: median = $0.151 \mu\text{m}^2/\text{s}$, IQR = 0.062 – $0.259 \mu\text{m}^2/\text{s}$, $n = 434$; AM281: median = $0.164 \mu\text{m}^2/\text{s}$, IQR = 0.086 – $0.255 \mu\text{m}^2/\text{s}$, $n = 785$; and WIN: median = $0.124 \mu\text{m}^2/\text{s}$, IQR = 0.008 – $0.227 \mu\text{m}^2/\text{s}$, $n = 194$; $P < 0.001$; Fig. 2C). We compared the diffusion coefficients of surface mobile receptors in vehicle versus treated cultures and found the different groups to be identical (control: median = $0.175 \mu\text{m}^2/\text{s}$, IQR = 0.088 – $0.272 \mu\text{m}^2/\text{s}$, $n = 396$; AM281: median = $0.175 \mu\text{m}^2/\text{s}$, IQR = 0.099 – $0.263 \mu\text{m}^2/\text{s}$, $n = 739$; and

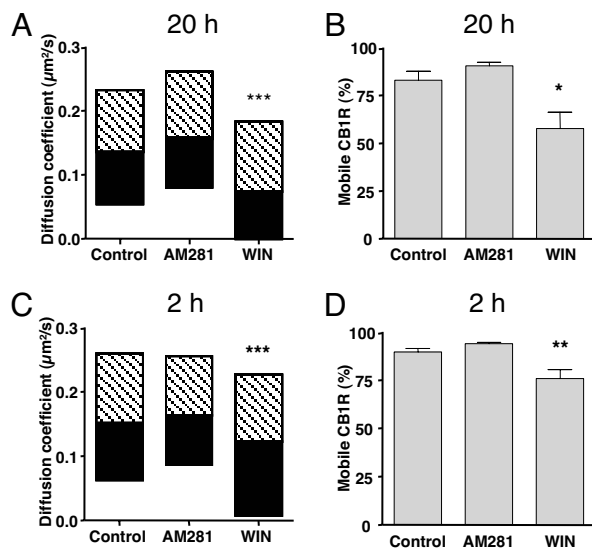


Fig. 2. Desensitization dramatically reduces the fraction of mobile CB1Rs. (A) Twenty hours of treatment with the cannabinoid agonist WIN (400 nM) lowered the diffusion coefficients of surface CB1Rs. Summary graph of the distribution of diffusion coefficients of all CB1Rs after 20 h of treatment with vehicle (DMSO 0.1%; control $n = 369$); the CB1 antagonist AM281 (400 nM; $n = 808$); or the cannabinoid agonist WIN (400 nM; $n = 145$). Bar graph of medians and IQRs is shown (t test, $***, P < 0.001$). (B) Twenty hours of treatment with the cannabinoid agonist WIN (400 nM) profoundly reduced the number of mobile CB1Rs (t test, $*P < 0.05$); that is, $D > 0.005 \mu\text{m}^2/\text{s}$. In contrast, 20 h of treatment with the antagonist AM281 (400 nM) had no effect. (C) Two hours of treatment with the cannabinoid agonist significantly reduced the mobility of CB1Rs. Summary graph shows the distribution of diffusion coefficients of all CB1Rs after 2 h of treatment with vehicle (control), WIN, or AM281. Bar graph of medians and IQRs is shown (t test, $***, P < 0.001$). (D) Two hours of treatment with the cannabinoid agonist significantly reduced the fraction of mobile CB1Rs (t test, $**P < 0.01$); that is, $D > 0.005 \mu\text{m}^2/\text{s}$. Two hours of treatment with the antagonist AM281 (400 nM) had no effect (control $n = 434$, AM281 $n = 785$, and WIN $n = 194$ trajectories).

WIN: median = $0.169 \mu\text{m}^2/\text{s}$, IQR = $0.088\text{--}0.247 \mu\text{m}^2/\text{s}$, $n = 148$; $P > 0.05$). In contrast, the 2-h agonist treatment significantly reduced the percentage of mobile CB1Rs: in vehicle-treated cultures, $89.7\% \pm 1.7\%$ ($n = 434$) of CB1Rs were mobile, whereas after agonist exposure, this number dropped to $75.9\% \pm 4.7\%$ ($n = 194$; Fig. 2D). After short agonist treatment, the apparent reduction in the mobility was due to a decrease in the fraction of mobile receptors.

The Effects of the Cannabinoid Agonist Are Mediated by CB1Rs. We verified that CB1Rs mediate the effect of the CB agonist. Coincubation with the specific CB1R antagonist AM281 blocked the agonist-induced reduction of surface CB1R diffusion coefficients (control: median = $0.216 \mu\text{m}^2/\text{s}$, IQR = $0.036\text{--}0.415 \mu\text{m}^2/\text{s}$, $n = 1,174$; WIN: median = $0.030 \mu\text{m}^2/\text{s}$, IQR = $0.0003\text{--}0.319 \mu\text{m}^2/\text{s}$, $n = 617$; WIN plus AM281: median = $0.231 \mu\text{m}^2/\text{s}$, IQR = $0.101\text{--}0.379$, $n = 1,708$; $P < 0.001$; Fig. 3A). AM281 also blocked agonist-induced reduction of CB1R mobility (Fig. 3B): there were $75.5\% \pm 2.7\%$ ($n = 1,174$), $50.4\% \pm 4.4\%$ ($n = 617$), and $79.0\% \pm 5.0\%$ ($n = 1,708$) mobile receptors in control, WIN, and WIN plus AM281, respectively. Thus, CB1Rs mediate the effects of the CB agonist.

CB1R Desensitization Does Not Alter the Mobility of AMPARs. AMPARs underlie most of the excitatory currents at glutamatergic excitatory synapses, and we have studied extensively their movements on neuronal membranes (4, 5, 22, 23). We tested the impact of subchronic treatment with either the CB agonist or the

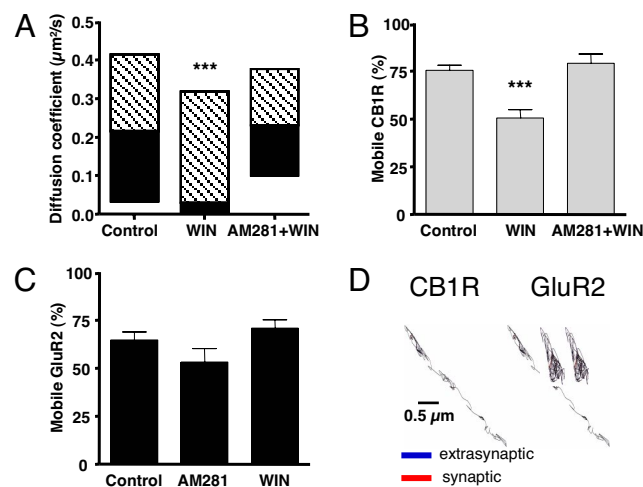


Fig. 3. CB1R specifically mediates cannabinoid-induced desensitization. (A) CB1Rs mediate the cannabinoid-induced reduction in the movements of surface CB1Rs after 20 h of agonist treatment. The effect of the cannabinoid agonist was abolished by coincubation with the specific CB1R antagonist AM281 (1 μM). Summary graph of the distribution of diffusion coefficients of all CB1Rs in control, WIN-treated, and WIN plus AM281-treated cultures. Bar graph of medians and IQRs is shown (t test, $***, P < 0.001$). (B) Twenty hours of treatment with the cannabinoid agonist WIN (400 nM) strongly reduced CB1R surface mobility. The specific CB1R antagonist AM281 (1 μM) prevented the effect of 20 h of treatment with the cannabinoid agonist (t test, $***, P < 0.001$); control $n = 1,174$, WIN $n = 617$, and WIN plus AM281 $n = 1,708$ trajectories. (C) The effects of the cannabinoid agonist were specific to CB1Rs: the lateral mobility of GluR2 subunits of AMPAR was not affected after 20 h of treatment with WIN (t test, $P > 0.05$); control $n = 694$, AM281 $n = 449$, and WIN $n = 470$ trajectories. (D) Example trajectories of CB1Rs and GluR2 subunits of AMPAR. Blue and red lines represent the extrasynaptic and the synaptic parts of the trajectories, respectively. (Scale bar, $0.5 \mu\text{m}$.)

CB1R antagonist on the mobility of GluR2-containing AMPARs. Such treatments had no effect on the mobility of GluR2-containing AMPARs (Fig. 3C and D), strongly suggesting that CB1R desensitization does not result in a general alteration of neurotransmitter receptor surface movements.

Desensitization Excludes CB1R from Synapses. During desensitization, the fraction of immobile receptors increased significantly. The synaptic terminal is composed of several subcompartments with different functional specialization (24). Are the CB1Rs within these compartments affected equally by agonist treatment? We compared the effects of CB1R desensitization on the mobility of CB1Rs in the extrasynaptic and synaptic compartments. Both 2 h and 20 h of agonist-induced desensitization reduced the fraction of synaptic CB1Rs (Fig. 4A). Agonist treatment reduced by as much as 60% the fraction of synaptic CB1Rs. In vehicle-treated neurons, 3% of CB1Rs ($\pm 0.6\%$, $n = 434$) were in synapses. Less than 1% of CB1Rs ($0.7\% \pm 0.2\%$, $n = 194$) remained within synapses after 2 h of agonist treatment. The CB1R antagonist AM281 had no effect on the number of synaptic receptors ($2.9\% \pm 0.6\%$, $n = 785$). There were $3.8\% \pm 0.8\%$ ($n = 369$), $2.9\% \pm 0.6\%$ ($n = 808$), and $1.3\% \pm 0.9\%$ ($n = 145$) synaptic receptors after 20 h of vehicle, AM281, and WIN treatment, respectively. Thus, agonist exposure caused a remarkable reduction in synaptic CB1Rs.

To determine whether the synaptic residency time and the exchange of CB1Rs between synaptic and extrasynaptic compartments altered by CB1R desensitization, we quantified the synaptic dwell time of CB1R agonist-treated cultures. Twenty hours of WIN treatment did not change the residency time of CB1Rs in the synapse (control: dwell time = 0.2 ± 0.05 s, $n =$

diffusive movement within the synaptic and extrasynaptic compartments. The short synaptic dwell time of CB1Rs compared with postsynaptic AMPARs (12, 13) may be due to intrinsic receptor properties, differences in anchoring, and interacting partner proteins, and more generally to the marked structural differences in presynaptic and postsynaptic specializations. In accord with the concept that receptor dynamics reflect the features of their immediate surroundings, extrasynaptic (i.e., axonal) CB1R behaviors indicated free diffusive movement, whereas CB1Rs displayed more confined movement within the spatially restricted synaptic domain.

Desensitization Has an Impact on CB1R Mobility. During chronic consumption of cannabis derivatives, such as marijuana, CB1Rs show a marked tolerance (17–19). Desensitized CB1Rs are internalized via the clathrin-coated pit pathway. The dynamics of the CB1Rs that remain on the neuronal surface after desensitization have never been explored. We found that a reduction in the mobility of CB1Rs reflects agonist-induced desensitization. This effect was due to a massive increase in the fraction of immobile CB1Rs and not a global reduction in the diffusion of mobile CB1Rs, showing that agonist-induced desensitization controls discrete features of CB1R dynamics.

Desensitization Excludes Surface CB1Rs from the Synaptic Terminal. The eCB system is a retrograde signaling system where eCBs produced in the postsynapse cross the synaptic cleft, bind to presynaptic CB1Rs, and inhibit transmitter release (3). A unique *in vivo* exposure to Δ^9 -tetrahydrocannabinol causes a reversible loss of CB1R function that is not due to CB1R internalization or uncoupling (8, 16). The present data identify a mechanism allowing synapses to efficiently reduce CB1R response after agonist activation. Desensitization was accompanied by a marked increase in the fraction of immobile receptors and a selective decrease in the diffusion coefficients of extrasynaptic CB1Rs. The data show that desensitized CB1Rs are gradually slowed down and immobilized in the extrasynaptic zone, resulting in a progressive loss of synaptic CB1Rs. The functional characteristics of immobilized CB1Rs are unknown, but an exciting hypothesis is that they are incompetent in signaling. In all cases, it is likely that receptors outside the synapse receive fewer signaling eCBs than their synaptic counterparts.

Conclusions

Our data shed light on the dynamic behavior of native presynaptic CB1Rs and suggest that subtle regulations of CB1R movements participate in the complex molecular cascade underlying agonist-induced desensitization. The presently revealed mechanism has significant implications for the study of mechanisms underlying tolerance of other presynaptic GPCRs.

Materials and Methods

Cortical Cell Culture. Cultures of cortical neurons were prepared from Swiss mice (Janvier). On the day of birth the pups were killed by cervical dislocation under isoflurane anesthesia. Dissected cortices were dissociated with the use of papain and were finally triturated mechanically. Cells were plated at a density of 360,000 cells per ml and grown on poly-L-lysine-coated coverslips in MEM supplemented with Serum Supreme (BioWhittaker).

Pharmacological Treatments. The reagents were added to the culture medium 30 min, 2 h, or 20 h before the experiment at the following concentrations: 400 nM WIN and 400 nM AM281, DMSO (1:1,000).

Immunocytochemistry. For live surface CB1R staining, neurons were briefly rinsed in PBS (160 mM NaCl, 10 mM Hepes, 10 mM glucose, 2.4 mM KCl, and 1.5 mM CaCl₂) and incubated for 15 min with polyclonal antibodies raised against the N terminus of the CB1 receptor (1:1,000; gift from K. Mackie, Indiana University, Bloomington, IN), fixed with 4% paraformaldehyde, permeabilized with 0.1% Triton X-100, bathed in a blocking buffer (0.5% BSA in PBS), and then incubated overnight at 4°C with the other primary antibodies diluted in blocking buffer. After washing, cells were incubated with secondary antibodies for 90 min, washed, and mounted on glass coverslips with Aqua-PolyMount (Polysciences). Polyclonal CB1R antibodies were visualized with Alexa 488-conjugated anti-rabbit IgG (Invitrogen). The monoclonal anti-MAP2 (1:500), anti-Tau1 (1:500), and anti-GAD65 (1:500) antibodies were revealed with an Alexa 568-conjugated anti-mouse IgG.

Microscopy. Micrographs of immunolabeling with MAP2, Tau1, and GAD65 antibodies were acquired with an epifluorescence microscope (Leica DMR video microscope; oil immersion 40×, N.A. 1.25 objective). Single-particle tracking was performed at 32°C with an inverted microscope (Olympus IX71) equipped with an oil immersion 100×, N.A. 1.35 objective. QDots and MitoTracker were illuminated with a mercury lamp (Olympus) and detected by using appropriate excitation (HQ560/55, HQ480/40) and emission (D655/20, HQ535/50) filters (Chroma Technology). A total of 1,500 consecutive frames were acquired at 20 Hz with an EM-CCD camera QuantEM (20 Hz) or with a CCD camera CoolSNAP_{HQ} (2.5 Hz; Figs. 2 and 4A) (Photometrics).

Single-Particle (Qdot) Tracking. Polyclonal CB1R N-terminus-specific antibodies were incubated with QDot 655 F(ab')₂ anti-rabbit (Thermo Fisher Scientific) in PBS for 2 h. The incubation was then blocked with casein for 30 min. CB1R antibodies coupled to QDots655 (CB1R-QD655) were filtered through a column of Superdex 200 gel (Amersham Biosciences). The same protocol was applied for monoclonal anti-GluR2 antibodies (Chemicon) coupled with QDot 655 F(ab')₂ anti-mouse.

Neurons were incubated with CB1R-QD655 or GluR2-QD655 for 10 min at 37°C, washed, and incubated for 1 min with a synaptic marker MitoTracker (20 nM; Invitrogen). After the final wash, coverslips were mounted in a chamber with permanent perfusion of a recording medium (160 mM NaCl, 10 mM Hepes, 10 mM glucose, 2.4 mM KCl, and 1.5 mM CaCl₂). To avoid recording of internalized CB1Rs, all of the movies were taken within 20 min. Control experiments performing acid stripping (pH 2.8, 4 min, 4°C) did not show internalized CB1R-QD655 after 20 min of incubation (data not shown) (34).

Trajectory Analysis. The CB1R-QD655 or GluR2-QD655 recording sessions were processed with MetaMorph software (Universal Imaging). As previously described (12), the spatial distribution of the signals of the CCD is fitted to a 2-dimensional Gaussian surface. The 2-dimensional trajectories of single molecules in the plane of focus were constructed by correlation analysis between consecutive images using a Vogel algorithm. Tracking of single QDots was performed with custom software written with Matlab (Mathworks). The MSD was calculated according to $\langle r^2 \rangle = [\sum_{j=1}^{N-n} (X_{i+n} - X_i)^2 + (Y_{i+n} - Y_i)^2] / (N - n) dt$ for reconnected trajectories. The diffusion coefficient (D) was calculated from linear fits of the first 4 points of MSD curves versus time using $MSD(t) = \langle r^2 \rangle (t) = 4Dt$. To assign synaptic localization, trajectories were sorted into extrasynaptic and synaptic by using the mitochondria marker MitoTracker image (9–11): MitoTracker-positive pixels defined the synaptic zone (11). Synapse dwell time was calculated as a mean residency time of CB1R-QD655 within synapses. All of the trajectories of CB1R that did not leave the synapse during the imaging period were excluded.

ACKNOWLEDGMENTS. We thank Dr. P. Chavis for discussions and the imaging system. We thank Dr. J. Blahos and members of O.J.M.'s laboratory for their support, P. Legros and C. Pujol from the Plate-forme d'Imagerie Cellulaire de l'Institut des Neurosciences de Bordeaux imaging center for their technical support, and Dr. M. Sepers for reading the manuscript. This work was supported by grants from the Institut National de la Santé et de la Recherche Médicale, the Fondation pour la Recherche Médicale, Région Aquitaine, and Agence Nationale de Recherche Neurologie et Psychiatrie Grant ANR-06-NEUR-043-01. L.M. was supported by the French Embassy in the Czech Republic, the Fondation pour la Recherche Médicale, ENI-Net, and the Czech Republic Grants GACR 204/05/0920 and GACR 309/03/H095.

- Piomelli D (2003) The molecular logic of endocannabinoid signalling. *Nat Rev Neurosci* 4:873–884.
- Mackie K (2007) From active ingredients to the discovery of the targets: The cannabinoid receptors. *Chem Biodivers* 4:1693–1706.
- Chevalleyre V, Takahashi KA, Castillo PE (2006) Endocannabinoid-mediated synaptic plasticity in the CNS. *Annu Rev Neurosci* 29:37–76.

- Groc L, Choquet D (2006) AMPA and NMDA glutamate receptor trafficking: Multiple roads for reaching and leaving the synapse. *Cell Tissue Res* 326:423–438.
- Triller A, Choquet D (2005) Surface trafficking of receptors between synaptic and extrasynaptic membranes: And yet they do move! *Trends Neurosci* 28:133–139.
- Jin W, et al. (1999) Distinct domains of the CB1 cannabinoid receptor mediate desensitization and internalization. *J Neurosci* 19:3773–3780.

7. Wu DF, et al. (2008) Role of receptor internalization in the agonist-induced desensitization of cannabinoid type 1 receptors. *J Neurochem* 104:1132–1143.
8. Mato S, et al. (2004) A single in-vivo exposure to Δ^9 THC blocks endocannabinoid-mediated synaptic plasticity. *Nat Neurosci* 7:585–586.
9. Groc L, et al. (2007) Surface trafficking of neurotransmitter receptor: Comparison between single-molecule/quantum dot strategies. *J Neurosci* 27:12433–12437.
10. Groc L, et al. (2004) Differential activity-dependent regulation of the lateral mobilities of AMPA and NMDA receptors. *Nat Neurosci* 7:695–696.
11. Tardin C, Cognet L, Bats C, Lounis B, Choquet D (2003) Direct imaging of lateral movements of AMPA receptors inside synapses. *EMBO J* 22:4656–4665.
12. Bats C, Groc L, Choquet D (2007) The interaction between Stargazin and PSD-95 regulates AMPA receptor surface trafficking. *Neuron* 53:719–734.
13. Ehlers MD, Heine M, Groc L, Lee MC, Choquet D (2007) Diffusional trapping of GluR1 AMPA receptors by input-specific synaptic activity. *Neuron* 54:447–460.
14. Groc L, Choquet D (2008) Measurement and characteristics of neurotransmitter receptor surface trafficking [review]. *Mol Membr Biol* 25:344–352.
15. Hoffman AF, Oz M, Caulder T, Lupica CR (2003) Functional tolerance and blockade of long-term depression at synapses in the nucleus accumbens after chronic cannabinoid exposure. *J Neurosci* 23:4815–4820.
16. Mato S, Robbe D, Puente N, Grandes P, Manzoni OJ (2005) Presynaptic homeostatic plasticity rescues long-term depression after chronic Δ^9 -tetrahydrocannabinol exposure. *J Neurosci* 25:11619–11627.
17. Lichtman AH, Martin BR (2002) Marijuana withdrawal syndrome in the animal model. *J Clin Pharmacol* 42:205–275.
18. Lichtman AH, Martin BR (2005) Cannabinoid tolerance and dependence. *Handb Exp Pharmacol* 168:691–717.
19. Gonzalez S, Cebeira M, Fernandez-Ruiz J (2005) Cannabinoid tolerance and dependence: A review of studies in laboratory animals. *Pharmacol Biochem Behav* 81:300–318.
20. Coutts AA, et al. (2001) Agonist-induced internalization and trafficking of cannabinoid CB1 receptors in hippocampal neurons. *J Neurosci* 21:2425–2433.
21. Leterrier C, et al. (2006) Constitutive activation drives compartment-selective endocytosis and axonal targeting of type 1 cannabinoid receptors. *J Neurosci* 26:3141–3153.
22. Choquet D, Triller A (2003) The role of receptor diffusion in the organization of the postsynaptic membrane. *Nat Rev Neurosci* 4:251–265.
23. Heine M, et al. (2008) Surface mobility of postsynaptic AMPARs tunes synaptic transmission. *Science* 320:201–205.
24. Schoch S, Gundelfinger ED (2006) Molecular organization of the presynaptic active zone. *Cell Tissue Res* 326:379–391.
25. Mackie K (2006) Cannabinoid receptors as therapeutic targets. *Annu Rev Pharmacol Toxicol* 46:101–122.
26. Malinow R, Malenka RC (2002) AMPA receptor trafficking and synaptic plasticity. *Annu Rev Neurosci* 25:103–126.
27. McDonald NA, Henstridge CM, Connolly CN, Irving AJ (2007) An essential role for constitutive endocytosis, but not activity, in the axonal targeting of the CB1 cannabinoid receptor. *Mol Pharmacol* 71:976–984.
28. Leterrier C, Bonnard D, Carrel D, Rossier J, Jenkei Z (2004) Constitutive endocytic cycle of the CB1 cannabinoid receptor. *J Biol Chem* 279:36013–36021.
29. Mundigl O, et al. (1993) Synaptic vesicle proteins and early endosomes in cultured hippocampal neurons: Differential effects of brefeldin A in axon and dendrites. *J Cell Biol* 122:1207–1221.
30. Parton RG, Simons K, Dotti CG (1992) Axonal and dendritic endocytic pathways in cultured neurons. *J Cell Biol* 119:123–137.
31. Irving AJ, et al. (2000) Functional expression of cell surface cannabinoid CB(1) receptors on presynaptic inhibitory terminals in cultured rat hippocampal neurons. *Neuroscience* 98:253–262.
32. Nyiri G, Cserep C, Szabadits E, Mackie K, Freund TF (2005) CB1 cannabinoid receptors are enriched in the perisynaptic annulus and on preterminal segments of hippocampal GABAergic axons. *Neuroscience* 136:811–822.
33. Groc L, et al. (2007) NMDA receptor surface trafficking and synaptic subunit composition are developmentally regulated by the extracellular matrix protein Reelin. *J Neurosci* 27:10165–10175.
34. Fourgeaud L, et al. (2003) The metabotropic glutamate receptor mGluR5 is endocytosed by a clathrin-independent pathway. *J Biol Chem* 278:12222–12230.

Supporting Information

Mikasova et al. 10.1073/pnas.0805959105

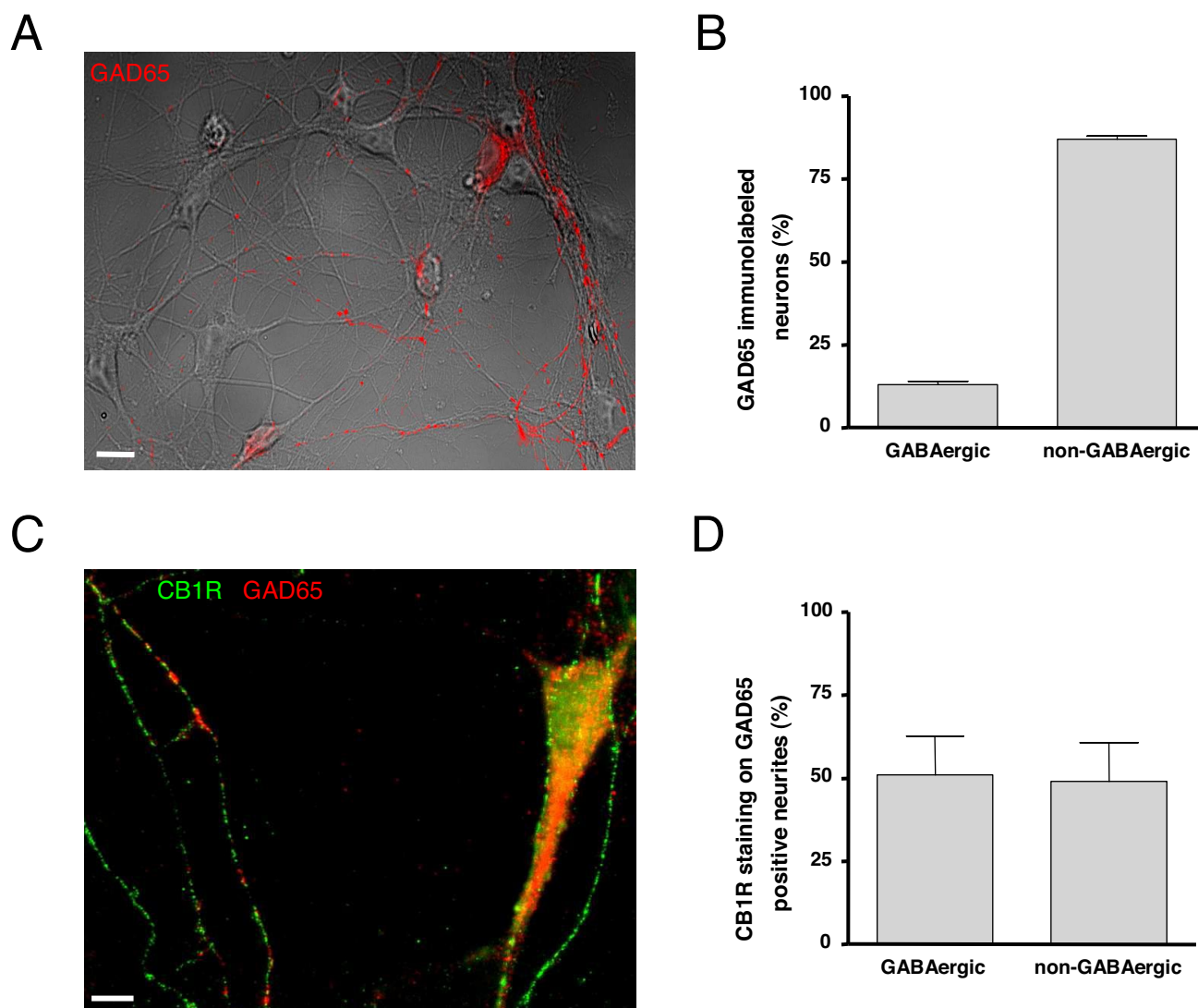
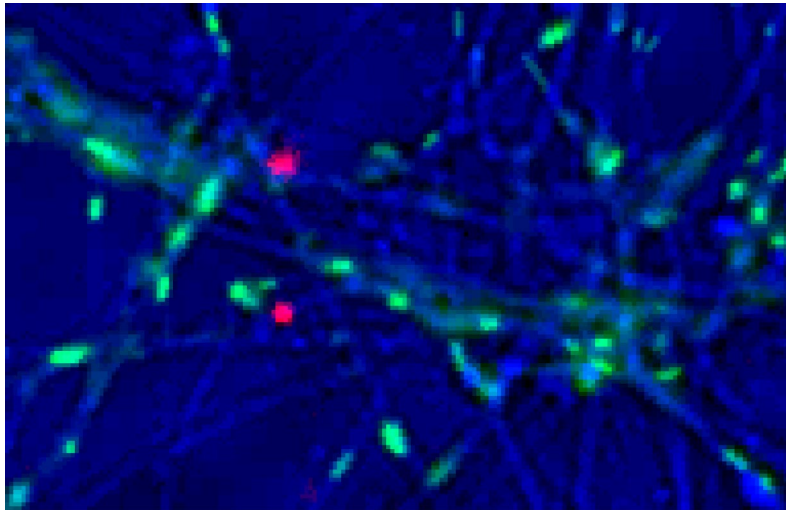


Fig. S1. In cortical neuronal cultures, CB1Rs are expressed in both GABAergic and non-GABAergic neurons. (A) Illustrative image of the overlay of GAD65 immunoreactivity and bright-field image. (Scale bar, 10 μm .) (B) Quantification of percentage of GAD65-positive neurons calculated from 3 independent experiments ($n = 603$). (C) Illustrative image of overlay of GAD65 (red) and CB1R (green) immunoreactivity. (Scale bar, 6 μm .) (D) Quantification of percentage of CB1Rs detected on GAD65-positive neurites calculated from 4 independent experiments ($n = 89$).



— Synapses (MitoTracker®)
— CB1R-Qdot655

Movie S1. CB1R lateral mobility on the surface of cortical neurons. Sample video of lateral mobility of CB1R coupled with Quantum dot (CB1R-QD655). Synapses were visualized by an active mitochondrial marker (MitoTracker, green); CB1R-QD655 (red).

[Movie S1 \(AVI\)](#)